Dyes and Pigments 86 (2010) 32–41

Contents lists available at ScienceDirect

Dyes and Pigments

journal homepage: www.elsevier.com/locate/dyepig

Fluorescent macromolecular perylene diimides containing pyrene or indole units in bay positions

Haluk Dinçalp [a,*], Şevki Kızılok [a], Sıddık İçli [b]

[a] Department of Chemistry, Faculty of Art and Science, Celal Bayar University, Muradiye 45030, Manisa, Turkey
[b] Solar Energy Institute, Ege University, Bornova, 35100 Izmir, Turkey

ARTICLE INFO

Article history:
Received 13 September 2009
Received in revised form
26 November 2009
Accepted 28 November 2009
Available online 11 December 2009

Keywords:
Perylene diimide
Pyrene
Solvatochromism
Charge transfer
HOMO–LUMO energy levels
DSSC

ABSTRACT

Novel, symmetric and unsymmetric perylene diimide dyes with pyrene or indole units in the bay positions of the perylene ring were synthesized and characterized using FT-IR, ^{1}H and ^{13}C NMR, MS, UV-Vis spectra and cyclic voltammetry. The λ_{max} in different solvents were in the range 526–585 nm and emission wavelengths of the dyes exhibited positive solvatochromism with increasing solvent polarity. Long wavelength emissions >750 nm of dyes with pyrene units displayed charge-separated state of perylene–pyrene system. Dyes with pyrene or indole units showed greater photostability in toluene than dyes which did not contain these bulky substituents. Incorporating electron-donating indole substituents lowered the band gap energies and, therefore, the HOMO energy levels were increased. The energy density and shape of the molecular orbitals were calculated theoretically.

1. Introduction

From a multifunctional perspective, perylene diimides (PDI) have received much attention and are widely used in many applications owing to their high fluorescence quantum yield [1–3], large molar absorption coefficient [3,4], high photo- and thermal stabilities under visible light irradiation [5–7], high chemical stability [8] and ease of their tunable absorption properties [9,10]. Both symmetric and unsymmetric derivatives of diimides have been extensively used in dye sensitized solar cells (DSSC) [11–14], organic light emitting diodes (OLED) [15], organic field effect transistors (OFED) [16], liquid crystal displays (LCD) [17], dye lasers [18], photosensitizers in chemical oxidations [7], photodynamic therapy [19] and DNA G-quadruplex stabilization [20–22].

Many attempts have been made to enhance the light harvesting properties and to improve the photophysical properties of PDIs. Photoinduced energy and electron transfer processes in multichromophoric PDI systems containing electron-donating and electron-withdrawing groups are crucial point in the field of material science, especially in the fabrication of DSSCs. In these cells, an electron acceptor–donor system is required to enhance the life time of charge-separated state which contributes to charge accumulation at resembling electrodes and then to photocurrent generation. In recent articles, to obtain new dyes having stronger intramolecular charge transfer and more promising absorptive properties, PDIs have been functionalized at the 1- and 7-positions using substituents which are suitable for solar light conversion [23–26]. Absorption spectra of the synthesized dyes have to cover the entire visible region of solar spectra to enhance the cell efficiency. Also, the energy distribution of HOMO/LUMO levels of dyes is significant subject for charge separation and charge injection processes in DSSCs. If the HOMO/LUMO orbital separation is strong on the same molecule, charge injection occurs immediately from excited state of dye to the conduction band of metal oxide. Thus, the photovoltaic performance of dye will be better.

This paper concerns the participation of electron donor, pyrene or indole moieties, in the electron-acceptor perylene core for improving solar cell efficiency. The synthetic routes are shown in Schemes 1 and 2 for the preparation of the perylene series (**P** dyes).

2. Experimental

2.1. General procedures

^{1}H NMR (400 MHz) and ^{13}C spectra (100 MHz) were recorded by a Bruker spectrometer. FT-IR spectra were recorded on a Perkin Elmer-Spectrum BX spectrophotometer on KBr pellets. LC/MS

* Corresponding author. Tel.: +90 236 2412151/2543; fax: +90 236 2412158.
E-mail address: haluk.dincalp@bayar.edu.tr (H. Dinçalp).

0143-7208/$ – see front matter © 2009 Elsevier Ltd. All rights reserved.
doi:10.1016/j.dyepig.2009.11.005

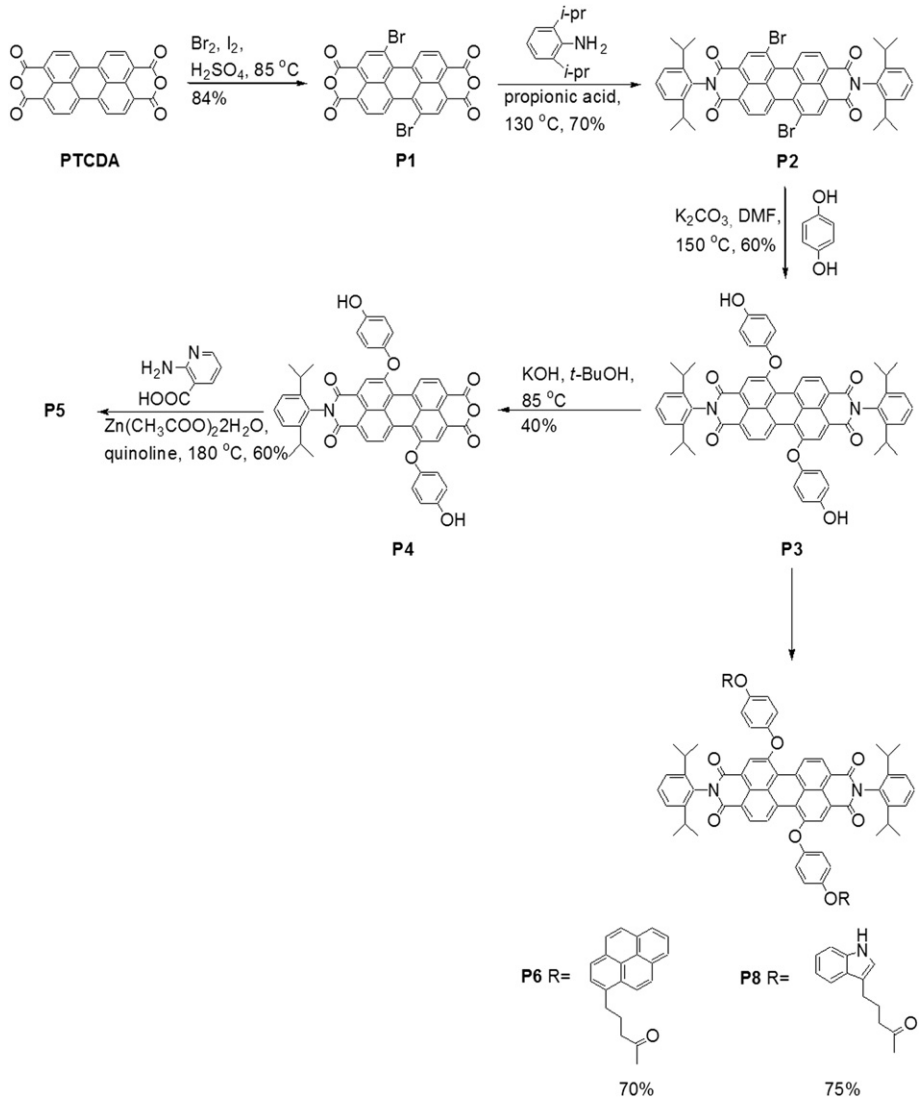

Scheme 1. Synthesis of the perylene diimide dyes **P6** and **P8**.

analyses were performed with an Agilent 1100 MSD instrument. The collision energies in positive and negative ion mode were determined at 55 eV and 70 eV, respectively. UV-Vis spectra were taken on an Analytic Jena Speedcord S-600 diode-array spectrophotometer in the solutions. Fluorescence properties of the synthesized compounds were obtained using a PTI QM1 fluorescence spectrophotometer. Their fluorescence quantum yields were calculated with reference to fluorescence emission of perylene-3,4,9,10-tetracarboxylic-bis-N,N′-dodecyl diimide ($\Phi_F = 1.0$ in chloroform, $\lambda_{exc} = 485$ nm) [27] and to fluorescence emission of pyrene ($\Phi_F = 0.32$ in cyclohexane, $\lambda_{exc} = 317$ nm) [28]. The fluorescence decay times were taken on a sub-nanosecond pulsed LEDs. Details on the time-resolved measurements were reported elsewhere [22]. Optical density of the solutions which were used in the spectroscopic studies was below 0.1. Cyclic and differential pulse voltammetry studies of the **P** dyes were performed with a CH instruments (Electrochemical Workstation) and a potentiostat in a three electrode single-compartment cell which was controlled by a computer. Surface of glassy carbon electrode which was used as working electrode was polished prior to use in order to obtain reproducible surfaces. Platinum and Ag/Ag^+ electrodes were used as counter and reference electrodes, respectively. The supporting electrolyte was 100 mM [TBA][PF6] in Me-CN. All dyes were prepared in spectrophotometric grade Me-CN. All potentials were internally referenced to the ferrocene–ferrocenium couple which was exhibited at about +0.54 V. Redox potentials of the dyes were calculated from reversible waves with the formula $[E_{p(ox)} + E_{p(red)}]/2$.

Molecular mechanics optimization of dye molecules was achieved by MM+ force field and the HOMO–LUMO orbital surfaces were calculated by ZINDO/S (Single Point/CI) using Hyperchem Package Version 8.0 computational software.

The following chemical reagents were purchased and used without further purification: perylene-3,4,9,10-tetracarboxylic dianhydride (Fluka), bromine (Merck), iodine (Merck), 2,6-diisopropylaniline (Aldrich), propionic acid (Laboratory BDH Reagent), hydroquinone (Merck), 2-aminonicotinic acid (Abcr Gmbh), $Zn(CH_3COO)_2\ 2H_2O$ (Carlo Erba), 1-pyrene butyric acid (Merck), N,N′-dicyclohexylcarbodiimide (Aldrich), 4-dimethylaminopyridine (Acros Organics), *p*-toluenesulfonic acid monohydrate (Fluka), indole-3-butyric acid (Aldrich). Other chemical reagents and organic solvents were analytical grade and used without further purification. To investigate the solvent dependent kinetics of the dye solutions, all dyes were studied in five

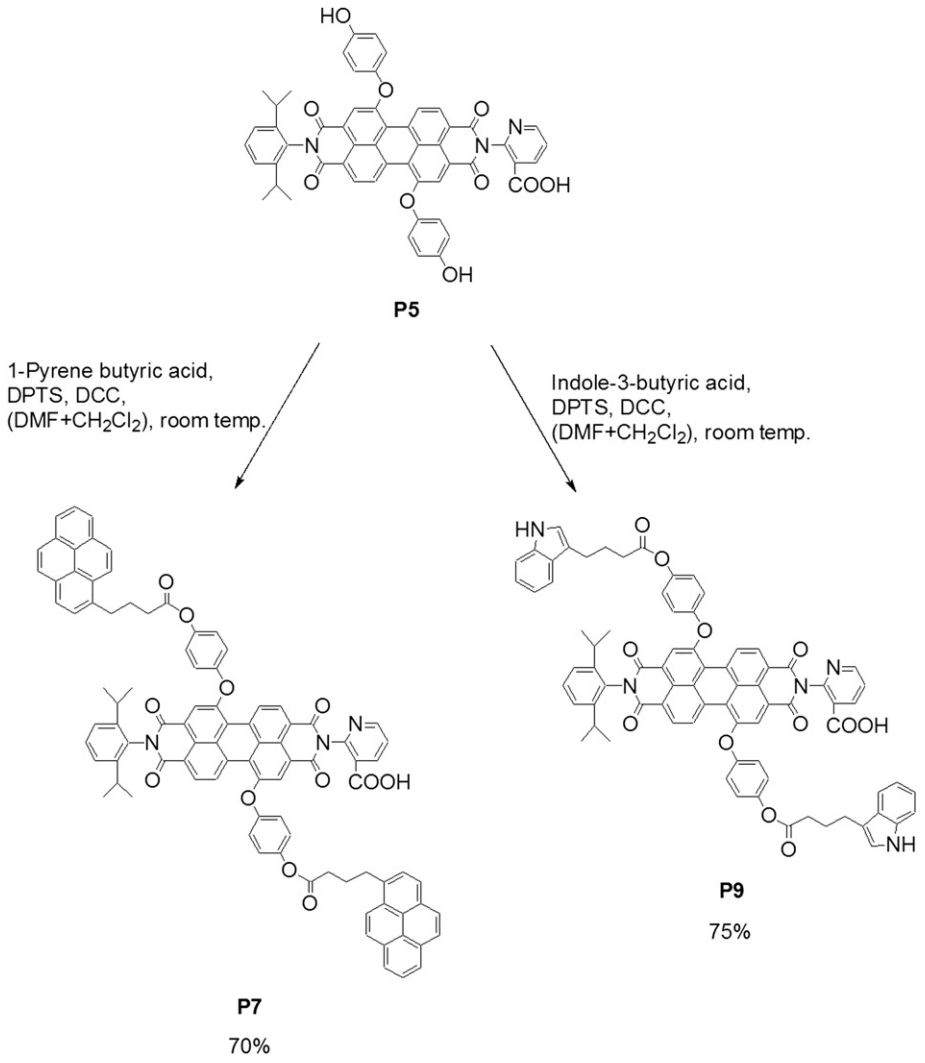

Scheme 2. Synthesis of **P7** and **P9** dyes from **P5**.

different solvents ranging from low to high polarity. These solvents were toluene (ε = 2.4), chloroform (ε = 4.8), methanol (ε = 32.7), acetonitrile (ε = 35.9), and PBS (ε = 80.2) [29] and spectroscopic grade.

2.2. Synthesis

2.2.1. Synthesis of 1,7-dibromo-perylene-3,4,9,10-tetracarboxylic dianhydride (*P1*)

Following the published procedure [30], a 500 mg (0.91 mmol) sample of perylene-3,4,9,10-tetracarboxylic dianhydride (PTCDA) was dissolved in 4 mL of conc H_2SO_4. The solution was stirred at room temperature under an air atmosphere for 16 h. Iodine (11.8 mg, 46.5 μmol) and 144 μL (2.81 mmol) of bromine were added to the solution. The solution was heated to 85 °C for 10 h with stirring. The mixture was cooled to room temperature, and the product was isolated by filtration and washed with water until the pH of the solution was reached to about 7. The crude product was purified by column chromatography on silica gel using $CHCl_3$:CH_3COOH (48:2) as an eluent to give the product as light red solid. $C_{24}H_6Br_2O_6$, Yield: 84%, FT-IR (KBr, cm^{-1}): 3119 (aromatic ν_{C-H}), 1770 ($\nu_{C=O}$), 1761 ($\nu_{C=O}$), 1594 (aromatic $\nu_{C=C}$), 1507, 1406, 1301 (ν_{C-O}), 1235, 1122, 1024, 860, 733 cm^{-1}. ^{1}H NMR [400 MHz, $CDCl_3$, δ 7.25 ppm]: δ = 9.58 (2H, d, J = 7.8 Hz, perylene H), 8.98 (2H, s, perylene H), 8.78 (2H, d, J = 7.8 Hz, perylene H) ppm.

2.2.2. Synthesis of N,N′-bis(2,6-diisopropylphenyl)-1,7-dibromoperylene-3,4,9,10-tetracarboxylic diimide (*P2*)

Following the published procedure [31], a solution of **P1** (150 mg, 0.17 mmol) in 10 mL of propionic acid was treated with 2,6-diisopropylaniline (224 μL, 1.1 mmol). The reaction mixture was stirred at 130 °C under a nitrogen atmosphere for 26 h. The hot solution was filtered and the crude product was purified by column chromatography on silica gel using *n*-hexane:ethyl acetate:acetic acid (35:13:2) as an eluent to give the product as bordeaux solid. $C_{48}H_{40}Br_2N_2O_4$, Yield: 70%, FT-IR (KBr, cm^{-1}): 2962 (aliphatic ν_{C-H}), 2924 (aliphatic ν_{C-H}), 2868 (aliphatic ν_{C-H}), 1711 ($\nu_{C=O}$), 1672 ($\nu_{C=O}$), 1590 (aromatic $\nu_{C=C}$), 1465, 1386 (ν_{C-N}), 1335, 1240, 1198, 1144, 835 cm^{-1}. ^{1}H NMR [400 MHz, $CDCl_3$, δ 7.25 ppm]: δ = 9.57 (2H, d, J = 7.8 Hz, perylene H), 9.02 (2H, s, perylene H), 8.81 (2H, d, J = 7.8 Hz, perylene H), 7.51 (2H, t, J = 7.8 Hz, benzene H), 7.37 (4H, d, J = 7.8 Hz, benzene H), 2.74 (4H, septet, J = 7.0 Hz), 1.20 (24H, d, J = 7.0 Hz) ppm. ^{13}C NMR [100 MHz, $CDCl_3$, δ 77.5 ppm (3 peaks)]: 162.6 (C=O), 145.8, 138.6, 133.4, 130.8, 130.3, 130.0, 129.8, 128.9, 124.3, 123.4, 121.4, 121.2, 29.5 (**C**H(CH_3)$_2$), 24.1 (CH(**C**H_3)$_2$) ppm. LC/MS (ESI) m/z (%) = 871 (4), 870 (3), MI peak 869 [M^+] (5), 314 (35), 286 (43), 258 (24), 230 (15), 202 (100), 102 (10).

*2.2.3. Synthesis of N,N′-bis(2,6-diisopropylphenyl)-1,7-bis (4-hydroxyphenoxy)perylene-3,4,9,10-tetracarboxylic diimide (**P3**)*

A mixture of 0.70 g (0.81 mmol) **P2**, 0.74 g (6.72 mmol) of hydroquinone and 1.09 g (7.88 mmol) dry K_2CO_3 in 30 mL of dry DMF was reacted at 150 °C under an inert atmosphere for 1 h. After the mixture was cooled to room temperature, 30 mL of water was added to the solution. The precipitate was collected by suction filtration, and then washed with cold methanol–water solution. Chromatography on silica using chloroform:ethyl acetate (40:10) system afforded a purple solid. $C_{60}H_{50}N_2O_8$, Yield: 60%, FT-IR (KBr, cm^{-1}): 3329 (O–H stretching), 2963 (aliphatic ν_{C-H}), 2927 (aliphatic ν_{C-H}), 2869 (aliphatic ν_{C-H}), 1703 ($\nu_{C=O}$), 1654 ($\nu_{C=O}$), 1589 (aromatic $\nu_{C=C}$), 1505, 1447, 1406, 1364, 1337 (ν_{C-N}), 1258 (ν_{C-O}), 1190, 906, 838 cm^{-1}. ^1H NMR [400 MHz, $CDCl_3$, δ 7.25 ppm]: δ = 9.70 (2H, d, J = 8.6 Hz, perylene H), 8.72 (2H, d, J = 8.6 Hz, perylene H), 8.40 (2H, s, perylene H), 7.45 (2H, t, J = 7.8 Hz, benzene H), 7.31 (4H, d, J = 7.8 Hz, benzene H), 7.07 (4H, d, J = 8.6 Hz, phenol H), 6.87 (4H, d, J = 8.6 Hz, phenol H), 5.61 (2H, s, –OH), 2.73 (4H, septet, J = 7.0 Hz), 1.15 (24H, d, J = 7.0 Hz) ppm. ^{13}C NMR [100 MHz, $CDCl_3$, δ 77.0 ppm (3 peaks)]: 163.9 (C=O), 148.9, 147.8, 145.7, 142.5, 131.2, 130.5, 129.5, 128.5, 126.4, 125.4, 124.8, 124.0, 121.1, 119.7, 117.0, 116.7, 28.9 (**C**H$(CH_3)_2$), 24.0 (CH(**C**$H_3)_2$) ppm. LC/MS (ESI) m/z (%) = 928 (1), MI peak 927 [M^+] (2), 714 (20), 452 (63), 314 (18), 286 (18), 258 (11), 230 (16), 202 (100), 113 (26), 102 (11).

*2.2.4. Synthesis of N-(2,6-diisopropylphenyl)-1,7-bis(4-hydroxyphenoxy)perylene-3,4,9,10-tetracarboxylic 3,4-anhydride 9,10-imide (**P4**)*

Following the published procedure [32], the mixture of 0.16 g (0.17 mmol) **P3** and 0.064 g (1.14 mmol) of KOH in 40 mL of *t*-BuOH was reacted under reflux for 2 h. The reaction mixture was poured into a solution of 30 mL of AcOH and 15 mL of 2 N HCl. The resulting precipitate was collected by suction filtration, and then washed with dilute $NaHCO_3$ solution until the pH of the solution was reached to about 7. The crude product was purified by silica column chromatography eluted with $CHCl_3$:CH_3COOH (45:5). $C_{48}H_{33}NO_9$, Yield: 40%, FT-IR (KBr, cm^{-1}): 3310 (O–H stretching), 2963 (aliphatic ν_{C-H}), 2924 (aliphatic ν_{C-H}), 2851 (aliphatic ν_{C-H}), 1770 (anhydride $\nu_{C=O}$), 1734 (anhydride $\nu_{C=O}$), 1706 (imide $\nu_{C=O}$), 1658 (imide $\nu_{C=O}$), 1594 (aromatic $\nu_{C=C}$), 1504, 1448, 1406, 1348 (ν_{C-N}), 1258 (phenol ν_{C-O}), 1192 (anhydride ν_{C-O}), 1018 cm^{-1}. ^1H NMR [400 MHz, methanol-d_4, δ 4.80 (1) and 3.30 (5) ppm]: δ = 9.43 (2H, d, J = 8.6 Hz, perylene H), 8.54 (2H, d, J = 8.6 Hz, perylene H), 8.24 (2H, s, perylene H), 7.43 (1H, t, J = 7.8 Hz, benzene H), 7.32 (2H, d, J = 7.8 Hz, benzene H), 7.06 (4H, d, J = 7.8 Hz, phenol H), 6.87 (4H, d, J = 7.8 Hz, phenol H), 2.69 (2H, septet, J = 7.0 Hz), 1.13 (6H, d, J = 7.0 Hz), 1.11 (6H, d, J = 7.0 Hz) ppm. ^{13}C NMR [100 MHz, acetone-d_6, δ 206.3 (single peak) and 29.3 ppm (7 peaks)]: 163.3 (C=O), 162.8 (C=O), 159.6, 157.2, 156.3, 155.7, 147.1, 146.9, 146.2, 134.3, 132.9, 131.4, 130.0, 129.5, 129.1, 128.9, 126.6, 124.6, 123.9, 123.7, 123.3, 122.0, 121.6, 119.5, 117.3, 117.2, 28.7 (**C**H$(CH_3)_2$), 23.6 (CH(**C**$H_3)_2$), 13.7 (CH(**C**$H_3)_2$) ppm. LC/MS (ESI) m/z (%) = 769 (4), MI peak 768 [M^+] (7), 543 (10), 452 (11), 314 (52), 286 (64), 258 (41), 230 (39), 202 (100), 113 (12), 102 (16).

*2.2.5. Synthesis of N-(2,6-diisopropylphenyl)-N′-(3-carboxy-2-pyridyl)-1,7-bis(4-hydroxyphenoxy)perylene-3,4,9,10-tetracarboxylic diimide (**P5**)*

A mixture of 35 mg **P4** (45.6 μmol), 20 mg (144.8 μmol) 2-aminonicotinic acid and 3 mg (13.7 μmol) $Zn(CH_3COO)_2 \cdot 2H_2O$ was stirred in 5 mL of quinoline at 180 °C under a nitrogen atmosphere for 18 h. The reaction mixture was poured into a solution of 10 mL of Me-OH and 10 mL of 2 N HCl. The resulting precipitate was collected by suction filtration, and then washed with dilute Na_2CO_3 solution (10%) under vacuum. The crude product was purified by column chromatography on silica gel using chloroform:ethyl acetate:methanol (40:8:2) as an eluent. $C_{54}H_{37}N_3O_{10}$, Yield: 60%, FT-IR (KBr, cm^{-1}): 3523 (carboxylic acid O–H stretching), 3450, 3310 (phenol O–H stretching), 2957 (aliphatic ν_{C-H}), 2924 (aliphatic ν_{C-H}), 2868 (aliphatic ν_{C-H}), 1700 (imide $\nu_{C=O}$), 1664 (carboxylic acid $\nu_{C=O}$), 1653 (imide $\nu_{C=O}$), 1627, 1588 (aromatic $\nu_{C=C}$), 1502, 1404, 1337 (ν_{C-N}), 1258 (phenol ν_{C-O}), 1188 (carboxylic acid ν_{C-O}), 1068, 973, 808, 744, 553 cm^{-1}. ^1H NMR [400 MHz, $CDCl_3$, δ 7.19 ppm]: δ = 9.60 (2H, d, J = 8.6 Hz, perylene H), 9.55 (1H, d, J = 7.8 Hz, pyridine H), 8.69 (1H, d, J = 8.6 Hz, perylene H), 8.59 (1H, d, J = 8.6 Hz perylene H), 8.30 (1H, d, J = 7.8 Hz, pyridine H), 8.27 (1H, s, perylene H), 8.17 (1H, s, perylene H), 7.38 (1H, t, J = 7.8 Hz, benzene H), 7. 27 (1H, s, pyridine H), 7.24 (2H, d, J = 7.8 Hz, benzene H), 6.98 (4H, d, J = 8.6 Hz, phenol H), 6.83 (4H, d, J = 8.6 Hz, phenol H), 2.68 (2H, septet, J = 7.0 Hz), 1.08 (6H, d, J = 7.0 Hz), 1.06 (6H, d, J = 7.0 Hz) ppm. ^{13}C NMR [100 MHz, methanol, δ 47.7 ppm (7 peaks)]: 163.7 (C=O), 163.1 (C=O), 162.3 (C=O), 156.1, 155.5, 155.3, 148.7, 146.4, 146.2, 138.7, 136.8, 133.3, 132.0, 130.5, 129.9, 129.3, 128.8, 124.9, 123.8, 123.3, 123.2, 121.6, 121.3, 116.8, 29.0 (**C**H$(CH_3)_2$), 23.1 (CH(**C**$H_3)_2$), 18.5 (CH(**C**$H_3)_2$) ppm. LC/MS (ESI) m/z (%) = 890 [$M^+ + 2$] (1), 871 (16), 383 (30), 382 (100), 368 (47), 314 (24), 286 (37), 258 (15), 249 (22), 230 (29), 128 (29).

*2.2.6. Synthesis of 4-(N,N-dimethylamino)pyridinium-4-toluenesulfonate (**DPTS**)*

Following the published procedure [33], a mixture of 0.1 g (0.82 mmol) 4-dimethylaminopyridine and 0.156 g (0.82 mmol) *p*-toluenesulfonic acid monohydrate was stirred in 10 mL of THF at room temperature for 30 min. The resulting precipitate was collected by suction filtration to give white solid. $C_{14}H_{18}N_2O_3S$, Yield: 90%, FT-IR (KBr, cm^{-1}): 3064 (aromatic ν_{C-H}), 2918 (aliphatic ν_{C-H}), 2789 (ν_{Ar-N^+-H}), 1647, 1600, 1563 (aromatic $\nu_{C=C}$), 1451, 1401, 1216 (asymmetrical $\nu_{S=O}$), 1158 (symmetrical $\nu_{S=O}$), 1118, 1029 and 1006 (simetrik ν_{S-O}), 816, 682, 567 cm^{-1}. ^1H NMR [400 MHz, methanol-d4, δ 4.82 (1) and 3.30 (5) ppm]: 8.07 (2H, d, J = 6.2 Hz, pyridine H), 7.70 (2H, d, J = 7.8 Hz, benzene H), 7.22 (2H, d, J = 7.8 Hz, benzene H), 6.95 (2H, d, J = 6.2 Hz, pyridine H), 3.21 (6H, s, Ar–N$(CH_3)_2$), 2.34 (3H, s, Ar–CH_3) ppm.

*2.2.7. Synthesis of N,N′-bis(2,6-diisopropylphenyl)-1,7-bis {4-[(4-pyrene-1-ylbutanoyl)oxy]phenoxy}perylene-3,4,9,10-tetracarboxylic diimide (**P6**)*

Following the published procedure [34], the mixture of 17 mg (18.3 mmol) **P3**, 27 mg (93.6 mmol) 1-pyrene butyric acid, 33 mg (0.11 mmol) **DPTS** and 67 mg (0.32 mmol) N,N′-dicyclohexylcarbodiimide (**DCC**) in dry DMF/CH_2Cl_2 [7.5 mL (1:2)] was reacted at room temperature under an inert atmosphere for 18 h. After the mixture was cooled to room temperature, 15–20 mL of methanol was added to the solution to precipitate the crude product. The product was collected by filtration and then purified by silica column chromatography eluted with chloroform:ethyl acetate (40:10) to give **P6**. $C_{100}H_{78}N_2O_{10}$, Yield: 70%, FT-IR (KBr, cm^{-1}): 3445, 3014, 2924 (aliphatic ν_{C-H}), 2862 (aliphatic ν_{C-H}), 1734 (ester $\nu_{C=O}$), 1700 (imide $\nu_{C=O}$), 1650 (imide $\nu_{C=O}$), 1558 (aromatic $\nu_{C=C}$), 1541, 1490, 1457, 1398, 1342 (ν_{C-N}), 1258 (phenol ν_{C-O}), 1177 (ester ν_{C-O}), 1104 (ester ν_{C-O}), 1048, 869, 822, 668 cm^{-1}. ^1H NMR [400 MHz, $CDCl_3$, δ 7.25 ppm]: δ = 9.57 (1H, d, J = 7.8 Hz, perylene H), 8.71 (1H, d, J = 7.8 Hz, perylene H), 8.43 (1H, s, perylene H), 8.32 (1H, s, perylene H), 8.30 (2H, d, J = 7.8 Hz, perylene H), 8.14 (10H, m, pyrene H), 8.02 (4H, s, pyrene H), 7.97 (2H, m, pyrene H), 7.87 (2H, m, pyrene H), 7.47 (2H, t, J = 7.8 Hz, benzene H), 7.32 (4H, d, J = 7.8 Hz, benzene H), 7.16 (4H, s, phenol H) 7.14 (4H, s, phenol H), 3.48 (2H, t, J = 7.0 Hz), 3.39 (1H, t, J = 7.8 Hz), 2.70 (7H, m), 2.46 (1H, t, J = 7.0 Hz), 2.29 (5H, m), 1.16 (12H, d, J = 6.8 Hz), 1.14 (12H, d, J = 6.8 Hz) ppm. ^{13}C NMR [100 MHz, $CDCl_3$, δ 77.3 ppm

(3 peaks)]: 171.7 (C═O), 163.3 (C═O), 154.6, 153.3, 147.8, 147.3, 145.6, 135.2, 131.3, 130.8, 130.0, 128.7, 127.4, 127.3, 126.7, 125.8, 125.0, 124.9, 124.7, 124.0, 123.9, 123.4, 123.1, 119.8, 119.5, 118.4, 49.0, 33.9, 29.2 (**C**H(CH_3)$_2$), 25.6 (CH(**C**H_3)$_2$), 24.9 (CH(**C**H_3)$_2$), 24.0 ppm. LC/MS (APCI, negative) m/z = 1466 [M − H]$^-$.

*2.2.8. Synthesis of N-(2,6-diisopropylphenyl)-N′-(3-carboxy-2-pyridyl)-1,7-bis{4-[(4-pyrene-1-ylbutanoyl)oxy]phenoxy}perylene-3,4,9,10-tetracarboxylic diimide (**P7**)*

Following the published procedure [34], the mixture of 10 mg (11.3 mmol) **P5**, 14 mg (48.6 mmol) 1-pyrene butyric acid, 17 mg (58.8 μmol) **DPTS** and 34 mg (0.16 mmol) **DCC** in dry DMF/CH_2Cl_2 [7.5 mL (1:2)] was reacted at room temperature under an inert atmosphere for 20 h. After the mixture was cooled to room temperature, 15–20 mL of methanol was added to the solution to precipitate the crude product. The product was collected by filtration and then purified by silica column chromatography eluted with chloroform:ethyl acetate (45:5) to give **P7**. $C_{94}H_{65}N_3O_{12}$, Yield: 70%, FT-IR (KBr, cm^{-1}): 3277 (carboxylic acid O–H stretching), 3210, 2963, 2924 (aliphatic ν_{C-H}), 2862 (aliphatic ν_{C-H}), 1759 (ester $\nu_{C=O}$), 1731 (carboxylic acid $\nu_{C=O}$), 1700 (imide $\nu_{C=O}$), 1667 (imide $\nu_{C=O}$), 1627, 1588 (aromatic $\nu_{C=C}$), 1496, 1404, 1337 (ν_{C-N}), 1317, 1261, 1180 (ester ν_{C-O}), 1124 (ester ν_{C-O}), 1060, 841, 805, 755, 668 cm^{-1}. ^{1}H NMR [400 MHz, $CDCl_3$, δ 7.24 ppm]: δ = 9.55 (1H, d, J = 8.6 Hz, perylene H), 9.51 (1H, d, J = 8.6 Hz, pyridine H), 8.70 (1H, d, J = 8.6 Hz, perylene H), 8.64 (1H, d, J = 8.6 Hz, perylene H), 8.41 (1H, s, perylene H), 8.36 (1H, s, pyridine H), 8.31 (1H, s, pyridine H), 8.28 (2H, s, perylene H), 8.11 (10H, m, pyrene H), 7.99 (4H, s, pyrene H), 7.95 (2H, t, J = 7.8 Hz, pyrene H), 7.87 (2H, d, J = 7.8 Hz, pyrene H), 7.46 (1H, t, J = 7.8 Hz, benzene H), 7.30 (2H, d, J = 7.8 Hz, benzene H), 7.14 (4H, s, phenol H), 7.12 (4H, s, phenol H), 3.46 (4H, t, J = 7.8 Hz), 2.71 (4H, m), 2.30 (6H, m), 1.16 (6H, d, J = 6.8 Hz), 1.15 (6H, d, J = 6.8 Hz) ppm. ^{13}C NMR [100 MHz, $CDCl_3$, δ 77.5 ppm (3 peaks)]: 171.9 (C═O), 163.5 (C═O), 163.2 (C═O), 162.9 (C═O), 155.0, 152.6, 147.6, 145.8, 135.5, 133.7, 131.6, 131.0, 130.8, 130.6, 130.2, 129.8, 128.9, 127.7, 127.6, 127.5, 127.4, 126.9, 126.0, 125.3, 125.1, 125.0, 124.5, 124.2, 123.7, 123.4, 122.8, 120.0, 119.9, 34.0, 32.8, 29.9 (**C**H(CH_3)$_2$), 26.8 (CH(**C**H_3)$_2$), 24.2 (CH(**C**H_3)$_2$), 14.3 ppm. LC/MS (APCI, negative) m/z (%) = 1429 [M − H]$^-$.

*2.2.9. Synthesis of N,N′-bis(2,6-diisopropylphenyl)-1,7-bis{4-[(4-indole-3-ylbutanoyl)oxy]phenoxy}perylene-3,4,9,10-tetracarboxylic diimide (**P8**)*

Following the published procedure [34], a solution of **P3** (10 mg, 10.8 μmol) in dry DMF/CH_2Cl_2 [6 mL (1:2)] was treated with indole-3-butyric acid (11 mg, 54.1 μmol) in the presence of **DPTS** (19 mg, 65.0 μmol) and **DCC** (39 mg, 0.19 mmol) at room temperature under an inert atmosphere overnight. Column chromatography using chloroform:ethyl acetate (45:5) on silica gave **P8**. $C_{84}H_{72}N_4O_{10}$, Yield: 75%, FT-IR (KBr, cm^{-1}): 3327, 2957, 2924 (aliphatic ν_{C-H}), 2851 (aliphatic ν_{C-H}), 1765 (ester $\nu_{C=O}$), 1703 (imide $\nu_{C=O}$), 1661 (imide $\nu_{C=O}$), 1627, 1591 (aromatic $\nu_{C=C}$), 1496, 1406, 1339 (ν_{C-N}), 1261 (phenol ν_{C-O}), 1180 (ester ν_{C-O}), 1116 (ester ν_{C-O}), 911, 741 cm^{-1}. ^{1}H NMR [400 MHz, $CDCl_3$, δ 7.25 ppm]: δ = 9.59 (2H, d, J = 8.6 Hz, perylene), 8.74 (2H, d, J = 8.6 Hz, perylene), 8.42 (1H, s, perylene), 8.35 (1H, s, perylene), 7.63 (2H, s, indole N–H), 7.46 (2H, t, J = 7.8 Hz, benzene), 7.32 (4H, d, J = 7.8 Hz, benzene), 7.19 (2H, d, J = 7.8 Hz, indole phenyl), 7.15 (2H, d, J = 3.1 Hz, indole phenyl), 7.13 (4H, s, phenol), 7.11 (4H, s, phenol), 7.08 (2H, d, J = 3.1 Hz, indole phenyl), 7.06 (2H, d, J = 7.8 Hz, indole phenyl), 7.01 (2H, s), 2.90 (4H, t, J = 7.0 Hz), 2.73 (4H, septet, J = 6.8 Hz), 2.62 (4H, t, J = 7.0 Hz), 2.18 (4H, pentet, J = 7.0 Hz), 1.16 (12H, d, J = 6.8 Hz), 1.14 (12H, d, J = 6.8 Hz) ppm. ^{13}C NMR [100 MHz, $CDCl_3$, δ 77.2 ppm (3 peaks)]: 170.8 (C═O), 163.6 (C═O), 157.5, 141.6, 137.5, 135.7, 135.1, 133.7, 131.0, 129.9, 127.6, 125.4, 125.0, 124.2, 123.7, 122.5, 122.2, 121.9, 119.9, 119.5, 119.0, 116.1, 115.4, 111.3, 34.1, 29.9, 29.4 (**C**H(CH_3)$_2$), 25.4, 24.7 (CH(**C**H_3)$_2$), 24.2 (CH(**C**H_3)$_2$) ppm.

*2.2.10. Synthesis of N-(2,6-diisopropylphenyl)-N′-(3-carboxy-2-pyridyl)-1,7-bis{4-[(4-indole-3-ylbutanoyl)oxy]phenoxy}perylene-3,4,9,10-tetracarboxylic diimide (**P9**)*

Following the published procedure [34], a solution of **P5** (10 mg, 11.2 μmol) in dry DMF/CH_2Cl_2 [6 mL (1:2)] was treated with indole-3-butyric acid (11 mg, 54.1 μmol) in the presence of **DPTS** (19 mg, 65.0 μmol) and **DCC** (39 mg, 0.19 mmol) at room temperature under an inert atmosphere overnight. Column chromatography using chloroform:ethyl acetate (45:5) on silica gave **P9**. $C_{78}H_{59}N_5O_{12}$, Yield: 75%, FT-IR (KBr, cm^{-1}): 3389 (carboxylic acid O–H stretching), 2963 (aliphatic ν_{C-H}), 2924 (aliphatic ν_{C-H}), 2868 (aliphatic ν_{C-H}), 1756 (ester $\nu_{C=O}$), 1728 (carboxylic acid $\nu_{C=O}$), 1704 (imide $\nu_{C=O}$), 1665 (imide $\nu_{C=O}$), 1591 (aromatic $\nu_{C=C}$), 1496, 1406, 1343 (ν_{C-N}), 1262, 1180 (ester ν_{C-O}), 1118 (ester ν_{C-O}), 906, 741 cm^{-1}. ^{1}H NMR [400 MHz, $CDCl_3$, δ 7.25 ppm]: δ = 9.63 (2H, d, J = 7.8 Hz, perylene), 9.58 (1H, s, pyridine), 8.70 (2H, d, J = 7.8 Hz, perylene), 8.42 (1H, s, pyridine), 8.39 (1H, s, pyridine), 8.01 (2H, s, perylene), 7.64 (2H, s, indole N–H), 7.47 (1H, t, J = 7.8 Hz, benzene), 7.33 (2H, d, J = 7.8 Hz, benzene), 7.19 (2H, d, J = 7.6 Hz, indole phenyl), 7.16 (2H, d, J = 7.6 Hz, indole phenyl), 7.14 (4H, s, phenol), 7.12 (4H, s, phenol), 7.10 (2H, d, J = 2.3 Hz, indole phenyl), 7.08 (2H, d, J = 2.3 Hz, indole phenyl), 7.01 (2H, s), 2.91 (4H, t, J = 7.0 Hz), 2.72 (2H, septet, J = 6.8 Hz), 2.63 (4H, t, J = 7.0 Hz), 2.18 (4H, pentet, J = 7.0 Hz), 1.16 (6H, d, J = 6.8 Hz), 1.15 (6H, d, J = 6.8 Hz) ppm. ^{13}C NMR [100 MHz, $CDCl_3$, δ 77.5 ppm (3 peaks)]: 172.2 (C═O), 163.5 (C═O), 161.9 (C═O), 161.7 (C═O), 155.6, 145.8, 136.7, 136.6, 133.7, 131.0, 130.0, 129.8, 127.6, 127.3, 126.1, 125.7, 124.9, 124.4, 124.2, 122.9, 122.2, 121.8, 120.2, 120.0, 119.5, 119.0, 115.7, 115.4, 115.3, 112.9, 111.3, 34.1, 29.9, 29.4 (**C**H(CH_3)$_2$), 25.4, 24.6 (CH(**C**H_3)$_2$), 24.2 (CH(**C**H_3)$_2$) ppm.

3. Results and discussion

3.1. Stationary and time-resolved measurements

The UV-Vis spectra of **P3**, **P6**, **P8** dyes in toluene are displayed in Fig. 1. Also, long wavelength absorption data of all **P** dyes are given in Table 1. All series of **P** dye show broad absorption band between wavelength of 450 and 625 nm which belongs to 0–0 transitions. A weak shoulder around 390 nm attributes to the π–π^* transition of

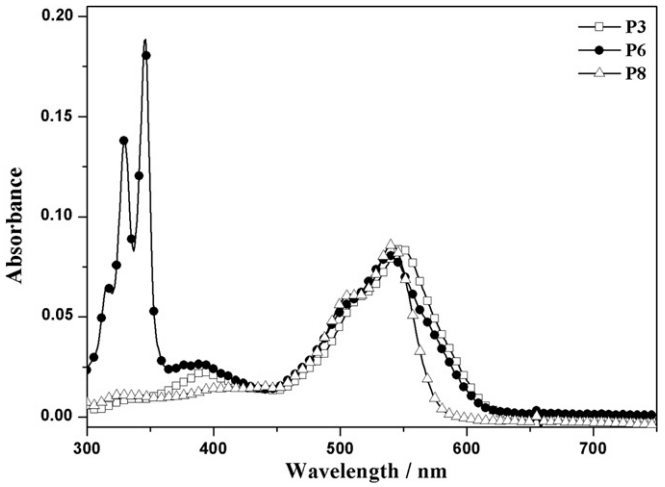

Fig. 1. UV-Vis absorption spectra of **P3**, **P6** and **P8** dyes in toluene at the concentrations of 10^{-6} M.

Table 1
Long wavelength absorption (λ/nm), emission maxima (λ_{em}/nm) and fluorescence quantum yields (Φ_F) of **P** dyes in five solvents of increasing polarity.

P dyes	Solvents													
	Toluene			Chloroform			Methanol			Acetonitrile			PBS[c], (pH 7.0)		
	λ	λ_{em}	Φ_F	λ	λ_{em}	Φ_F	λ	λ_{em}	Φ_F	λ	λ_{em}	Φ_F	λ	λ_{em}	Φ_F
P3	548	579	0.07[a]	548	578	0.08[a]	556	635	<0.01[a]	550	628	<0.01[a]	574	630	<0.01[a]
P5	547	576	0.17[a]	550	579	0.12[a]	553	565	<0.01[a]	548	566	<0.01[a]	585	615	<0.01[a]
P6	539	570	0.14[a] 0.14[b]	537	570	0.13[a] 0.09[b]	nd	nd	nd	540	573	0.04[a] 0.10[b]	567	640	<0.01[a] 0.06[b]
P7	539	566	0.26[a] 0.34[b]	540	571	0.25[a] 0.19[b]	nd	nd	nd	537	569	0.11[a] 0.23[b]	582	750	<0.01[a] 0.39[b]
P8	541	570	0.25[a]	540	571	0.32[a]	540	583	0.02[a]	537	575	0.08[a]	561	600	<0.01[a]
P9	539	562	0.27[a]	526	565	0.24[a]	nd	nd	nd	534	564	0.12[a]	566	605	<0.01[a]

nd: not determined.
[a] Fluorescence quantum yields have been determined using perylene-3,4,9,10-tetracarboxylic-bis-N,N′-dodecyl diimide (λ_{exc} = 485 nm).
[b] Fluorescence quantum yields have been determined using pyrene (λ_{exc} = 317 nm).
[c] PBS: 70 mM potassium phosphate/100 mM KCl/1 mM EDTA.

the aromatic rings. Three vibronic maxima at 345, 330 and 315 nm belong to the pyrene absorption for **P6** and **P7** dyes.

We have studied the optical properties of **P** dyes in different solvent of polarity. We choose low polar solvents such as toluene and chloroform, and high polar solvents such as methanol and acetonitrile. Also PBS, a more appropriate solution for biomedical applications of perylene diimides, is prepared and used in optical studies. In general, the absorption spectra of pyrene- or indole-substituted **P** dyes give a small hypsochromic shift of 3–4 nm in Me-CN compared to the corresponding spectra in toluene. This observation is explained by the low polarizability of excited state of the dyes in Me-CN. **P6**–**9** dyes do not effectively solvated in Me-OH because of their bulky aromatic groups which do not form hydrogen bond with Me-OH molecules. However, the absorption spectra of **P3** and **P5** dyes give a bathochromic shift of 3–4 nm in Me-OH with respect to the same spectra in toluene. This may be attributed to the formation of hydrogen bond between the solvent molecule and the non-bonding electrons of hydroxyl group attached to the benzene ring of the dyes [35]. The longest visible wavelength shift for all the dyes was observed in phosphate buffer solution among the studied solvents. Strong hydrogen bonding in buffer solution stabilizes the charge-transfer excited state so that absorption spectrum can shift to long-wavelength region [35].

Fig. 2 shows the solvent dependence of emission spectra of **P9** dye at the excitation wavelength of 485 nm. Contrary to the organic solvents, observed emission spectrum of **P9** in phosphate buffer solution is highly quenched and structureless. Also, it gives a marked red shift. This may be because the aggregation of the dye in solution. Also, excited state relaxation of **P9** dye in buffer solution leads to an increase in dipole moment. Moreover, much larger Stokes shift for **P** dyes is observed in higher polar solvents compared to lower polar solvents.

When **P7** dye in acetonitrile is excited at 317 nm, where the pyrene unit absorbs strongly, high energy radiation of pyrene monomer emission at 388 nm and low energy radiation of perylene unit emission at 569 nm are observed. In addition, new emission peaks around 758 and 788 nm appear (Fig. 3). Pyrenes are known to give monomer emission peaks below 400 nm [36] and efficient two excimer emission peaks between 440 and 480 nm [37]. No excimer emission of pyrene unit of the molecule is observed in Fig. 3. The red shifted emission peaks around 758 and 788 nm in the fluorescent emission spectrum of **P7** dye can be attributed to the formation of charge-separated states in donor–acceptor system. In comparison of the emission spectrum of the model compound **P5** dye in acetonitrile at the excitation wavelength of 485 nm, the compound gives the only emission from the perylene chromophore at 566 nm. If the only process upon the excitation of pyrene unit in **P7** dye is the energy transfer process, maximum of emission wavelength of the perylene unit should be the same as that of the model compound **P5** dye. Long wavelength emission peaks displayed in Fig. 3 are the direct spectroscopic evidences of the charge-separated state of **P7** dye in acetonitrile. Also, fast decay components obtained from the single photon counting experiments may be attributed to the formation of a charge transfer process in **P7** dye (Fig. 4 and Table 2). The same results are obtained

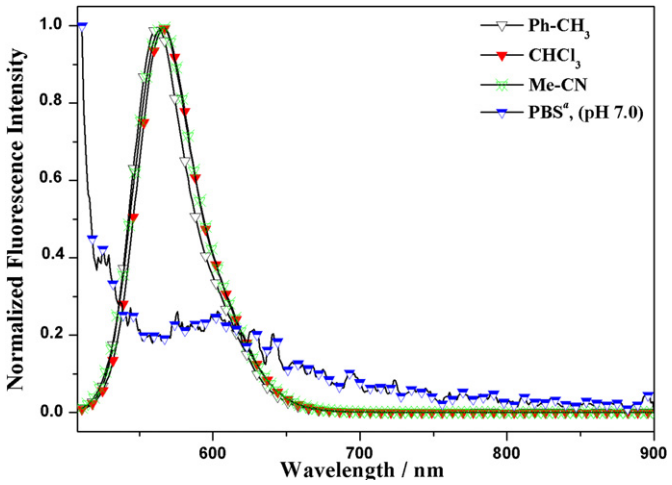

Fig. 2. The normalized fluorescence spectra of **P9** dye in different solvents of increasing polarity (λ_{exc} = 485 nm). [a]PBS: 70 mM potassium phosphate/100 mM KCl/1 mM EDTA.

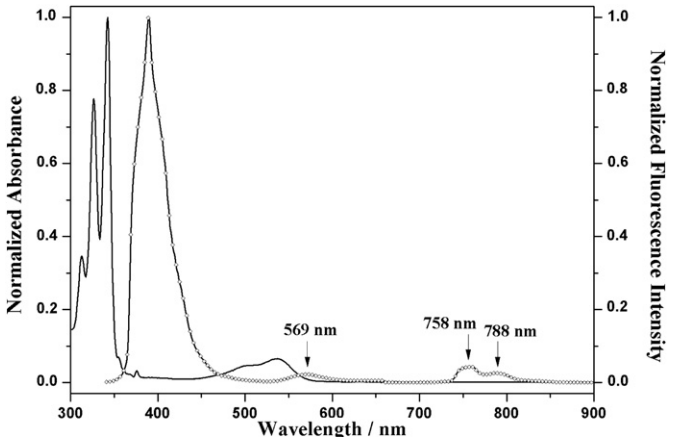

Fig. 3. The normalized UV-Vis absorption (with solid line) and fluorescence spectra (with symbol) of **P7** dye in Me-CN (λ_{exc} = 317 nm).

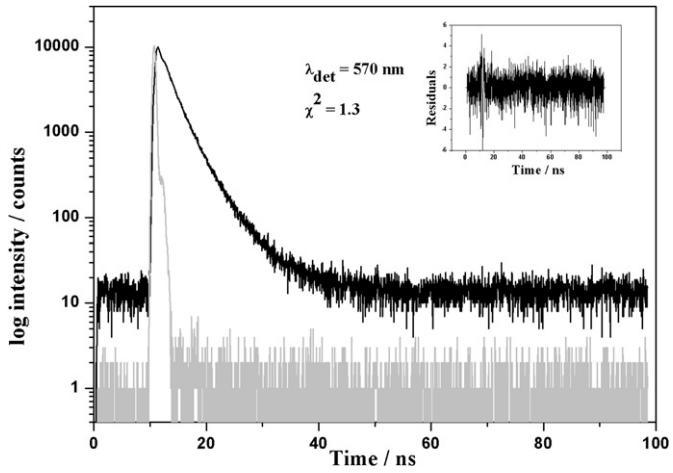

Fig. 4. Time-resolved fluorescence decay of **P7** in toluene. The inset shows the residuals. The time increment per channel amounts to be 42 ps.

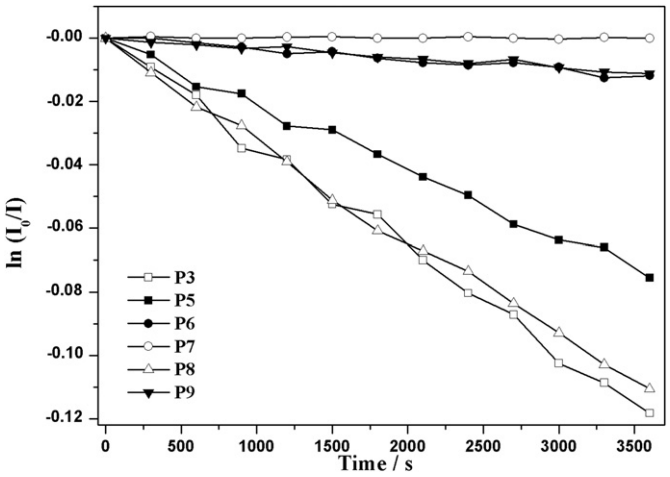

Fig. 5. Linear fits of the values obtained from the photodegradation curves of **P** dyes in toluene at the excitation wavelength of 254 nm for 1 h. Linear equations: **P3**: ($y = -3.3 \times 10^{-5}\cdot X - 1.9 \times 10^{-4}$; R^2: 0.99), **P5**: ($y = -2.1 \times 10^{-5}\cdot X - 2.7 \times 10^{-4}$; R^2: 0.99), **P6**: ($y = -3.5 \times 10^{-6}\cdot X + 3.1 \times 10^{-4}$; R^2: 0.96), **P8**: ($y = -3.0 \times 10^{-5}\cdot X - 0.00232$; R^2: 0.99), **P9**: ($y = -3.0 \times 10^{-6}\cdot X - 1.1 \times 10^{-4}$; R^2: 0.96).

in other studied solvents. Also, excitation of **P6** dye at 317 nm in the studied solvents gives the long wavelength emissions above 750 nm (data not shown). Photophysical properties of four bay-functionalized perylene diimides containing four attached pyrene moiety have been studied using time-resolved emission and femtosecond transient absorption in the literature [34,38]. Very fast photoinduced energy transfer as well as efficient electron transfer from the pyrene unit to the perylene diimide moiety has been detected in high yield.

Fluorescence quantum yields of **P6** and **P7** dye are higher than that of the model compounds **P3** and **P5** in the studied solvents at the excitation wavelength of 485 nm. This observation is explained by the conformational relaxation of the perylene diimide chromophore by introducing the pyrene or indole quenchers to the bay position of the ring. However, a significant quenching of pyrene emission in **P6** and **P7** dyes is observed as compared to the reference compound, pyrene itself ($\Phi_F = 0.32$ in cyclohexane). This behavior may be attributed to the formation of charge-separated state.

In single photon timing experiments, analysis of the decays revealed four-exponential decays at the emission wavelength of 570 nm for **P6**–**9** dyes in toluene as given in Table 2. The highest decay values for all the compounds may be attributed to the stationary fluorescence of perylene diimides. Fast decay components below 0.1 ns can be attributed to the photoinduced energy transfer or electron transfer between the perylene diimide chromophore and attached pyrene or indole moieties. As can be seen from the data given in Table 2, fluorescence rate constants of pyrene or indole-substituted perylene diimide dyes are higher than that of model compounds **P3** and **P5** dyes. This means that the HOMO level of the quencher lies below the HOMO level of perylene diimide. Electron transfer occurs only from excited states of pyrene moiety to the perylene diimide quencher.

Also, similar photophysical results have been observed for **P8** and **P9** dyes containing electron-withdrawing perylene diimide group and electron-releasing indole moieties. The absorption and emission spectra of both **P8** and **P9** dyes show similar blue shifts with respect to the model compounds **P3** and **P5** in the studied solvents. After introducing the indole quenchers into the phenol hydroxyl group of the model compounds **P3** and **P5**, n–π^* in the phenol backbone will decrease. Therefore, remarkable blue shifts were observed for **P8** and **P9** dye in the studied solvents. Fast decay components obtained with single photon timing experiments, high values of fluorescence rate constants and different emission maxima as compared to the model compounds indicate that photoinduced energy transfer as well as electron transfer occurs in the studied solvents for **P8** and **P9** dyes. Familiar compounds, perylene–benzoindole dyes, were synthesized for solar photovoltaic purposes in the literature [11]. Authors state that strong

Table 2
Fluorescence decay times (τ_f/ns), fluorescence lifetimes (τ_f/ns), radiative lifetimes (τ_0/ns), fluorescence rate constants ($k_f^r \times 10^8/s^{-1}$), non-radiative rate constants ($k^{nr} \times 10^8/s^{-1}$), and singlet energies (E_s/kcal mol^{-1}) of **P** dyes in toluene ($\lambda_{exc} = 485$ nm).[a]

P dyes	$\tau_{f(1)}$	$\tau_{f(2)}$	$\tau_{f(3)}$	$\tau_{f(4)}$	τ_f	τ_0	k_f^r	k^{nr}	E_s
P3	2.1	0.07	<0.01	–	0.7	10.4	1.0	12.8	52.9
P5	2.3	0.09	<0.01	–	0.8	4.7	2.1	10.4	53.0
P6	4.5	2.0	0.1	<0.01	1.7	11.2	0.8	5.2	53.8
P7	4.5	2.1	0.08	<0.01	1.7	6.4	1.6	4.4	53.8
P8	2.5	2.5	0.05	<0.01	1.3	5.1	2.0	5.9	53.6
P9	3.2	2.2	0.1	<0.01	1.4	5.1	2.0	5.3	53.8

[a] Photophysical parameters are calculated with the formulas: $\tau_f = \Sigma\tau_{f(n)}/n$, $\tau_0 = \tau_f/\Phi_F$, $k_f = 1/\tau_f = k_f^r + k^{nr}$, $k_f^r = 1/\tau_0$, $E_s = 0.0029/\lambda_{long} \times 10^{-7}$ [39,40].

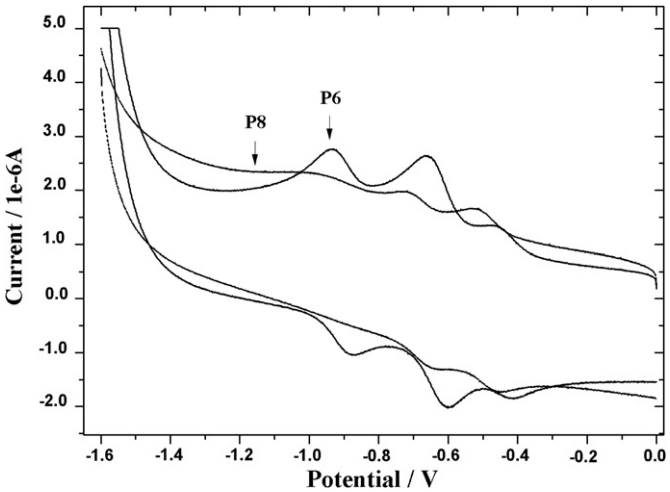

Fig. 6. CVs of the synthesized **P6** and **P8** dyes on glassy carbon working electrode in 0.1 M [TBA][PF6]/Me-CN at 500 mV/s scan rate.

Table 3
Cyclic voltammetry data for **P** dyes in 0.1 M [TBA][PF6]/Me-CN *vs.* Fc/Fc^{+} at 500 mV/s scan rate.

P dyes	E°_{red3} (V)	E°_{red2} (V)	E°_{red1} (V)	E°_{ox1} (V)	E°_{ox2} (V)	E°_{ox3} (V)
P1	–	−0.45	−0.21	1.02	–	–
P2	–	−0.50	−0.29	0.93	–	–
P3	−1.00	−0.71	−0.52	1.19	–	–
P4	–	−0.62	−0.44	1.34	–	–
P5	–	−0.69	−0.53	0.61	1.34	–
P6	−0.90	−0.63	−0.43	0.77	1.22	1.41
P7	–	−0.64	−0.47	0.82	1.30	1.63
P8	−0.94	−0.67	−0.48	0.56	1.13	1.62
P9	–	−0.65	−0.47	0.60	1.15	1.66

electron-withdrawing nature of these dyes transfers electrons under illumination towards the undesirable directions.

3.2. Photostability tests

Photostability of toluene solutions of all series of **P** dye were investigated. Specifically, toluene solutions were irradiated with Xe lamp exposure in fluorescence spectrophotometer at the excitation wavelength of 254 nm for 1 h. The emission data were collected at the emission wavelength of 570 nm. Photostability tests were performed with the detection of decrease in emission intensity at 570 nm. Photodegradation rate constants of the compounds were obtained from the slopes of the linear region of the semilogarithmic plot of for degradation decays of dyes *vs.* time [41], $\ln(I_0/I) = k_p \times t$. k_p values of **P3**, **P5**, **P6**, **P8**, and **P9** dyes were calculated to be 3.3×10^{-5}, 2.1×10^{-5}, 3.5×10^{-6}, 3.0×10^{-5}, 3.0×10^{-6}, respectively (Fig. 5). In general, it was understood from Fig. 5 that introducing the pyrene or indole units to the 1-, 7-bay positions of the perylene ring might enhance dye photostability.

3.3. CV measurements

It is important to get information about HOMO and LUMO energy levels of the series of **P** dye for solar cell applications. The electrochemical behavior of the dyes has been investigated by cyclic voltammetry. Fig. 6 gives the typical voltammograms of **P6** and **P8** dyes. The reduction and oxidation potentials were given in Table 3. Model compounds **P3** exhibits three reversible reduction waves ($E^{\circ}_{red1} = -0.52$ V, $E^{\circ}_{red2} = -0.71$ V, $E^{\circ}_{red3} = -1.00$ V) and one reversible oxidation wave ($E^{\circ}_{ox1} = 1.19$ V), indicating the formation of stable radical anions, dianions, trianions and radical cations of PDI, respectively. Symmetric **P6** and **P8** dyes give extra two oxidation peaks indicating the pyrene radical cations and indole radical cations, respectively.

Taking the reduction onsets into account, the LUMO energy levels have been calculated and listed in Table 4. The HOMO energy levels of **P6** and **P7** dyes containing pyrene moieties are calculated to be about −5.03 and −5.08 eV (1 eV = 1.602×10^{-19} J), respectively. This means that electron-rich pyrene derivatives improve the hole-injection capacity of the sensor dyes [42]. The corresponding LUMO energy levels are estimated to be −3.83 and −3.79 eV. The easy oxidation of **P8** and **P9** dyes at 0.56 and 0.60 eV suggests that the least electron-withdrawing capacity among the studied dyes is indole-substituted perylene diimides. The LUMO energy levels of all the above synthesized dyes are higher than the conduction band of TiO_2. Therefore, these dyes with appropriate molecular structures are suitable to n-type organic semiconductors for DSSCs.

Table 4
Molecular orbital energies[a] (eV) of **P** dyes with respect to the vacuum level.

P dyes	LUMO-2	LUMO-1	LUMO	HOMO	HOMO-1	HOMO-2	E_{gap2}	E_{gap1}	E_{gap}
P1	–	–	−4.05	−5.28	–	–	–	–	1.23
P2	–	–	−3.97	−5.19	–	–	–	–	1.22
P3	–	–	−3.74	−5.45	–	–	–	–	1.71
P4	–	–	−3.82	−5.60	–	–	–	–	1.78
P5	–	−3.57	−3.73	−4.87	−5.60	–	–	2.03	1.14
P6	−3.36	−3.63	−3.83	−5.03	−5.48	−5.67	2.31	1.85	1.20
P7	–	−3.62	−3.79	−5.08	−5.56	–	–	1.94	1.29
P8	−3.32	−3.59	−3.78	−4.82	−5.39	−5.88	2.56	1.80	1.04
P9	–	−3.61	−3.79	−4.86	−5.41	–	–	1.80	1.07

[a] HOMO and LUMO energy levels of the dyes were determined by the formulas: $E_{LUMO} = -(4.8 + E^{onset}_{red})$, $E^{onset}_{red} = E^{\circ}_{red} - E^{\circ}_{ox(ferrocene)}$, $E_{HOMO} = E_{LUMO} - E_{gap}$ [43].

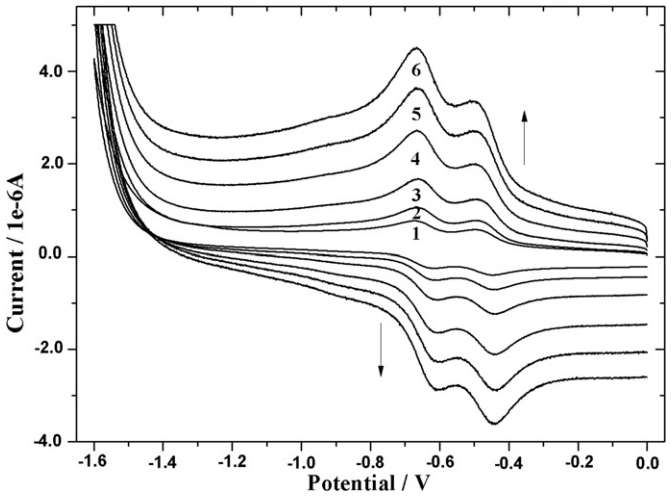

Fig. 7. CVs of **P7** dye on glassy carbon working electrode in 0.1 M [TBA][PF6]/Me-CN at 50 (1), 100 (2), 200 (3), 400 (4), 600 (5), and 800 (6) mV/s scan rates.

Fig. 7 shows the typical cyclic voltammograms of **P7** dye at various scan rates. The first and second reduction processes of **P7** dye, recorded at −0.47 and −0.64 V, could be assigned to (0/−1) and (−1/−2) species, respectively. ΔE_p values $[E_{p(anodic)} - E_{p(cathodic)}]$ changed from 48 to 58 mV with the scan rates ranging from 50 to 800 mV/s for **P7** dye. Also, **P7** dye gives a significant change at the peak current after 30 min electrolysis time as shown in Fig. 8. The cathodic redox potentials of **P7** dye show approximately 60 mV positive shift after 30 min electrolysis period with respect

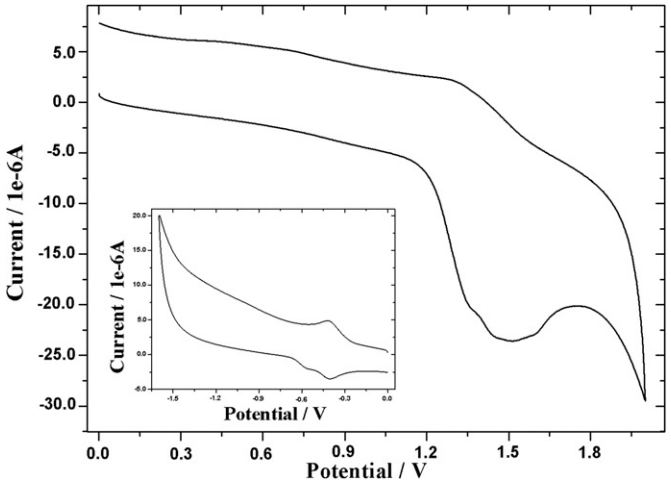

Fig. 8. Anodic and cathodic (inset) current peaks which were observed after 30 min electrolysis time for **P7** on glassy carbon working electrode in 0.1 M [TBA][PF6]/Me-CN at 500 mV/s scan rate.

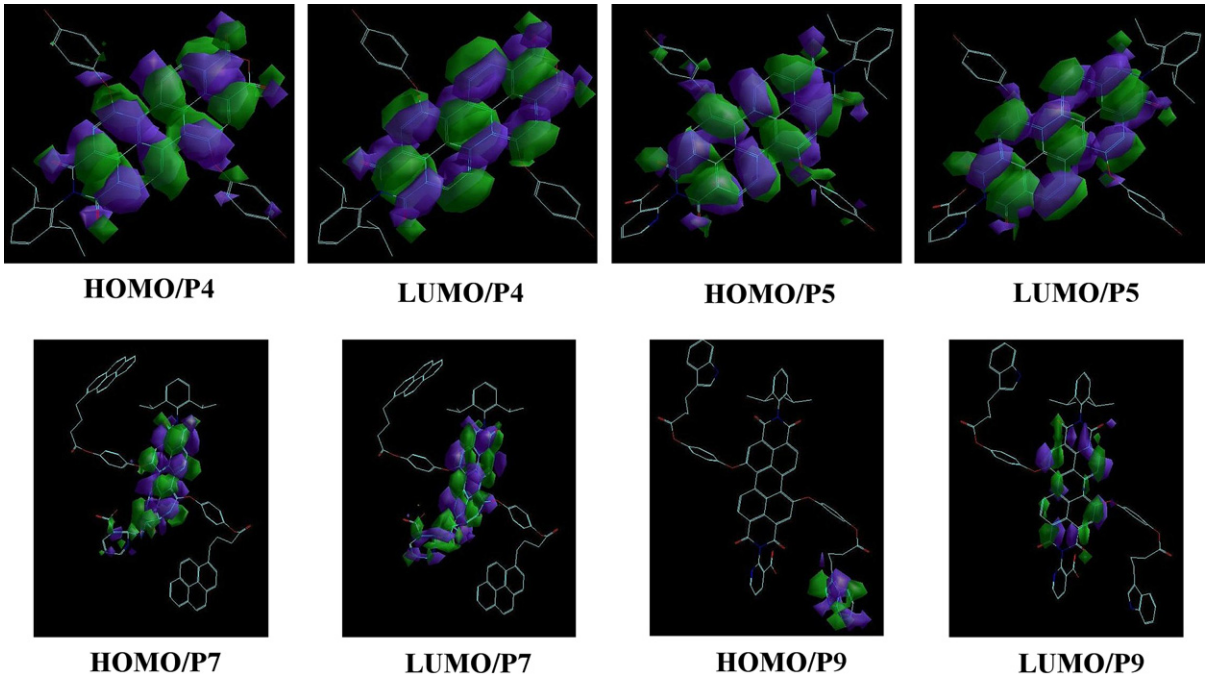

Fig. 9. Optimized structures and molecular orbitals of energy densities of **P4**, **P5**, **P7** and **P9** dyes.

to the initial time. Also, a significant negative shift from 1.63 V to 1.50 V is observed at anodic potential of **P7** dye at the end of the electrolysis time. First anodic peak observed at 0.82 V for **P7** dye was disappeared after 30 min electrolysis period. These shifts may be explained by the formation of charge transfer complex between the electron-donor pyrene and electron-acceptor perylene group of **P7** dye. No obvious change at the peak currents has been observed for indole-substituted perylene diimide dyes (**P8** and **P9**) and other model compounds.

Electron density diagrams for HOMO and LUMO orbitals of **P4**, **P5**, **P7** and **P9** dyes are depicted in Fig. 9. Both HOMO and LUMO orbitals of **P4**, **P5** and **P7** dyes are delocalized over the whole perylene ring. However, for **P9** dye containing perylene-indole group, HOMO level has the charge localized on the one of the indole rings while LUMO level has distributed along the perylene ring. These orbitals show a redistribution of the LUMO electron density predominantly in the acceptor perylene core of the studied compounds. HOMO orbitals of **P9** dye are distributed over the one of the indole groups which shows electron donating behavior. HOMO orbitals are delocalized generally on the donor site of the molecule, while LUMO orbitals are delocalized on the acceptor site of the molecule. Similar studies with frontier orbitals on perylene dyes have been studied in the literature and same explanations about the HOMO–LUMO orbital partitioning have been cited by the authors [10,44,45].

It is noted that bulky aromatic groups which show electron-releasing activity in the 1-, 7-bay positions slightly narrow the band gap energies with respect to the model compound **P3**. When the bay substituents of the perylene diimides are changed, HOMO energy levels increase while LUMO energy levels remain stable as compared to the model compound **P3**. These results are in well accordance with the literature data. Müllen and coworkers have studied the HOMO/LUMO energy tuning of perylene dyes based on N-(2,6-diisopropylphenyl)-perylene-3,4-dicarboximide and given the similar results about the effect of bay substituent on the HOMO/LUMO energy levels of the compounds [10]. An effective charge injection from the LUMO level of the dye to the conduction band of TiO_2 realizes in high efficiency PV materials when strong orbital partitioning occurs along the dye molecule [10,46].

4. Conclusions

We have synthesized and characterized new macromolecular perylene diimides. In a detailed photophysical analysis of the compounds, it is found that perylene diimide dyes containing pyrene or indole moieties show fast photoinduced energy transfer as well as efficient electron transfer from the quenchers to the perylene diimide moiety. Fast decay components, low fluorescence quantum yields at the excitation of pyrene quencher, long wavelength emission peaks and high values of fluorescence rate constants for **P7** dye support the formation of charge-separated states of **P7** dye in solution.

Also, negative and positive shifts at redox potentials are the evident for the formation of charge transfer complex between the electron-donor pyrene and electron-acceptor perylene groups of **P7** dye. In a simplified view, pyrene or indole units in the 1-, 7-bay positions slightly narrow the band gap energies and raise the HOMO energy level of the perylene diimides as compared to the model compound. For the indole-substituted perylene diimide, the HOMO orbital is localized on indole group while LUMO is extended on perylene core. Molecular structures of pyrene- or indole-substituted perylene diimides with appropriate LUMO energy values are suitable candidates for DSSCs.

Acknowledgements

This work was supported by the Research Council of Celal Bayar University (BAP/2007-006) and the State Planning Organization of Turkey (07 DPT 002).

References

[1] Kalinin S, Speckbacher M, Langhals H, Johansson LBA. A new and versatile fluorescence standard for quantum yield determination. Physical Chemistry Chemical Physics 2001;3:172–4.

[2] Langhals H, Kirner S. Novel fluorescent dyes by the extension of the core of perylenetetracarboxylic bisimides. European Journal of Organic Chemistry 2000;2:365–80.
[3] Langhals H, Karolin J, Johansson LBA. Spectroscopic properties of new and convenient standards for measuring fluorescence quantum yields. Journal of the Chemical Society, Faraday Transactions 1998;94:2919–22.
[4] Chao CC, Leung MK, Su YO, Chiu KY, Lin TH, Shieh SJ, et al. Photophysical and electrochemical properties of 1,7-diaryl-substituted perylene diimides. Journal of Organic Chemistry 2005;70(11):4323–31.
[5] Becker S, Böhm A, Müllen K. New thermotropic dyes based on amino-substituted perylendicarboximides. Chemistry A European Journal 2000;6 (21):3984–90.
[6] Nagao Y, Naito T, Abe Y, Misono T. Synthesis and properties of long and branched alkyl chain substituted perylenetetracarboxylic monoanhydride monoimides. Dyes and Pigments 1996;32(2):71–83.
[7] Dinçalp H, Içli S. Photoinduced electron transfer-catalyzed processes of sulfoamino perylene diimide under concentrated sun light. Solar Energy 2006;80:332–46.
[8] Karapire C, Zafer C, İçli S. Studies on photophysical and electrochemical properties of synthesized hydroxy perylenediimides in nanostructured titania thin films. Synthetic Metals 2004;145:51–60.
[9] Ego C, Marsitzky D, Becker S, Zhang J, Grimsdale AC, Müllen K, et al. Attaching perylene dyes to polyfluorene: three simple, efficient methods for facile color tuning of light-emitting polymers. Journal of the American Chemical Society 2003;125:437–43.
[10] Li C, Schöneboom J, Liu Z, Pschirer NG, Erk P, Herrmann A, et al. Rainbow perylene monoimides: easy control of optical properties. Chemistry A European Journal 2009;15:878–84.
[11] Jin Y, Hua J, Wu W, Ma X, Meng F. Synthesis, characterization and photovoltaic properties of two novel near-infrared absorbing perylene dyes containing benzo [e]indole for dye-sensitized solar cells. Synthetic Metals 2008;158:64–71.
[12] Zafer C, Kus M, Turkmen G, Dincalp H, Demic S, Kuban B, et al. New perylene derivative dyes for dye-sensitized solar cells. Solar Energy Materials and Solar Cells 2007;91:427–31.
[13] Aïch R, Ratier B, Tran-van F, Goubard F, Chevrot C. Small molecule organic solar cells based on phthalocyanine/perylene–carbazole donor–acceptor couple. Thin Solid Films 2008;516:7171–5.
[14] Mikroyannidis JA, Stylianakis MM, Roy MS, Suresh P, Sharma GD. Synthesis, photophysics of two new perylene bisimides and their photovoltaic performances in quasi solid state dye sensitized solar cells. Journal of Power Sources 2009;194(2):1171–9.
[15] Chiu TL, Chuang KH, Lin CF, Ho YH, Lee JH, Chao CC, et al. Low reflection and photo-sensitive organic light-emitting device with perylene diimide and double-metal structure. Thin Solid Films 2009;517:3712–6.
[16] Kim SH, Yang YS, Lee JH, Lee JI, Chu HY, Lee H, et al. Organic field-effect transistors using perylene. Optical Materials 2002;21:439–43.
[17] Cormier RA, Gregg BA. Synthesis and characterization of liquid crystalline perylene diimides. Chemistry of Materials 1998;10:1309–19.
[18] Sadrai M, Hadel L, Sauers RR, Husain S, Jespersen KK, Westbrook JD, et al. Lasing action in a family of perylene derivatives: singlet absorption and emission spectra, triplet absorption and oxygen quenching constants, and molecular mechanics and semiempirical molecular orbital calculations. Journal of Physical Chemistry 1992;96(20):7988–96.
[19] Yukruk F, Dogan AL, Canpinar H, Guc D, Akkaya EU. Water-soluble green perylenediimide (PDI) dyes as potential sensitizers for photodynamic therapy. Organic Letters 2005;7(14):2885–7.
[20] Fedoroff OY, Salazar M, Han H, Chemeris VV, Kerwin SM, Hurley LH. NMR-based model of a telomerase-inhibiting compound bound to G-quadruplex DNA. Biochemistry 1998;37(36):12367–74.
[21] Han H, Bennett RJ, Hurley LH. Inhibition of unwinding of G-quadruplex structures by Sgs1 helicase in the presence of N, N′-bis[2-(1-piperidino)ethyl]-3,4,9,10-perylenetetracarboxylic diimide, a G-quadruplex-interactive ligand. Biochemistry 2000;39:9311–6.
[22] Dincalp H, Avcıbası N, Icli S. Spectral properties and G-quadruplex DNA binding selectivities of a series of unsymmetrical perylene diimides. Journal of Photochemistry and Photobiology A 2007;185:1–12.
[23] Rybtchinski B, Sinks LE, Wasielewski MR. Combining light-harvesting and charge separation in a self-assembled artificial photosynthetic system based on perylenediimide chromophores. Journal of the American Chemical Society 2004;126:12268–9.
[24] Ishi-i T, Murakami Kİ, Imai Y, Mataka S. Light-harvesting and energy-transfer system based on self-assembling perylene diimide-appended hexaazatriphenylene. Organic Letters 2005;7(15):3175–8.
[25] Shibano Y, Umeyama T, Matano Y, Tkachenko NV, Lemmetyinen H, Imahori H. Synthesis and photophysical properties of electron-rich perylenediimide-fullerene dyad. Organic Letters 2006;8(20):4425–8.
[26] (a) Tauber MJ, Kelley RF, Giaimo JM, Rybtchinski B, Wasielewski MR. Electron hopping in π-stacked covalent and self-assembled perylene diimides observed by ENDOR spectroscopy. Journal of the American Chemical Society 2006;128:1782–3;
(b) Fan L, Xu Y, Tian H. 1,6-Disubstituted perylene bisimides: concise synthesis and characterization as near-infrared fluorescent dyes. Tetrahedron Letters 2005;46:4443–7;
(c) Pan JF, Zhu WH, Li SF, Xu J, Tian H. Synthesis of carrier-transporting dendrimers with perylenebis(dicarboximide)s as a luminescent. European Journal of Organic Chemistry 2006;4:986–1001;
(d) Gao B, Li Y, Tian H. Synthesis and near-infrared characteristics of novel perylene bisimide dyes bay-functionalized with naphthalimide chromophores. Chinese Chemical Letters 2007;18:283–6.
[27] Icli S, Icil H. A thermal and photostable reference probe for Qr measurements: chloroform soluble perylene 3,4,9,10-tetracarboxylic acid-bis-N, N′-dodecyl diimide. Spectroscopy Letters 1996;29(7):1253–7.
[28] Berlman IB. Handbook of fluorescence spectra of aromatic molecules. 2nd ed. New York: Academic Press; 1971.
[29] Scaiano JC. CRC handbook of organic photochemistry, vol. II. Florida: CRC Press Inc.; 1989.
[30] Böhm A, Arms H, Henning G, Blaschka P. 1,7-Diaroxy- or 1,7-arylthio-substituted perylene-3,4,9,10-tetracarboxylic acids, their dianhydrides and diimides. U.S. Patent 6,143,905; 2000.
[31] Liu Y, Li Y, Jiang L, Gan H, Liu H, Li Y, et al. Assembly and characterization of novel hydrogen-bond-induced nanoscale rods. Journal of Organic Chemistry 2004;69:9049–54.
[32] Wescott LD, Mattern DL. Donor–δ–acceptor molecules incorporating a non-adecyl-swallowtailed perylenediimide acceptor. Journal of Organic Chemistry 2003;68:10058–66.
[33] Xu K, Wang Y, Wang Y, Yu T, An L, Pan C, et al. Synthesis and characterization of ABC ternary segregated H-shaped copolymers. Polymer 2006;47: 4480–4.
[34] Kaletaş BK, Dobrawa R, Sautter A, Würthner F, Zimine M, Cola LD, et al. Photoinduced electron and energy transfer processes in a bichromophoric pyrene–perylene bisimide system. Journal of Physical Chemistry A 2004;108 (11):1900–9.
[35] Suppan P. Chemistry and light. London: The Royal Society of Chemistry; 1994. p. 77–86.
[36] Fujiwara Y, Amao Y. Optical oxygen sensor based on controlling the excimer formation of pyrene 1-butylic acid chemisorption layer onto nano-porous anodic oxidized aluminium plate by myristic acid. Sensors and Actuators, B 2003;89:58–61.
[37] Jun EJ, Won HN, Kim JS, Lee KH, Yoon J. Unique blue shift due to the formation of static pyrene excimer: highly selective fluorescent chemosensor for Cu^{2+}. Tetrahedron Letters 2006;47:4577–80.
[38] Sautter A, Kaletaş BK, Schmid DG, Dobrawa R, Zimine M, Jung G, et al. Ultrafast energy-electron transfer cascade in a multichromophoric light-harvesting molecular square. Journal of the American Chemical Society 2005;127: 6719–29.
[39] Suppan P. Chemistry and light. London: The Royal Society of Chemistry; 1994. p. 60–62.
[40] Turro NJ. Molecular photochemistry. London: Benjamin; 1965.
[41] Nombel LM, Matsuzawa S. Effect of solvents and a substituent group on photooxidation of fluorene. Journal of Photochemistry and Photobiology A 1998;119:15–23.
[42] Tang C, Liu F, Xia YJ, Lin J, Xie LH, Zhong GY, et al. Fluorene-substituted pyrenes – novel pyrene derivatives as emitters in nondoped blue OLEDs. Organic Electronics 2006;7:155–62.
[43] Pommerehne J, Vestweber H, Guss W, Mahrt RF, Bassler H, Porsch M, et al. Efficient 2-layer LEDs on a polymer blend basis. Advanced Materials 1995; 7(6):551–4.
[44] Zhang X, Wu Y, Li J, Li F, Li M. Synthesis and characterization of perylene tetracarboxylic bisester monoimide derivatives. Dyes and Pigments 2008;76: 810–6.
[45] Chiş V, Mile G, Ştiufiuc R, Leopold N, Oltean M. Vibrational and electronic structure of PTCDI and melamine–PTCDI complexes. Journal of Molecular Structure 2009;924–926:47–53.
[46] Tian H, Yang X, Chen R, Pan Y, Li L, Hagfeldt A, et al. Phenothiazine derivatives for efficient organic dye-sensitized solar cells. Chemical Communications 2007;36:3741–3.